



Fundamental efficiency bound for quantum coherent energy transfer in nanophotonics

CRISTIAN L. CORTES, WENBO SUN,  AND ZUBIN JACOB*

Birk Nanotechnology Center, Elmore Family School of Electrical and Computer Engineering, Purdue University, West Lafayette, Indiana 47907, USA

*zjacob@purdue.edu

Abstract: We derive a unified quantum theory of coherent and incoherent energy transfer between two atoms (donor and acceptor) valid in arbitrary Markovian nanophotonic environments. Our theory predicts a fundamental bound $\eta_{max} = \frac{\gamma_a}{\gamma_d + \gamma_a}$ for energy transfer efficiency arising from the spontaneous emission rates γ_d and γ_a of the donor and acceptor. We propose the control of the acceptor spontaneous emission rate as a new design principle for enhancing energy transfer efficiency. We predict an experiment using mirrors to enhance the efficiency bound by exploiting the dipole orientations of the donor and acceptor. Of fundamental interest, we show that while quantum coherence implies the ultimate efficiency bound has been reached, reaching the ultimate efficiency does not require quantum coherence. Our work paves the way towards nanophotonic analogues of efficiency-enhancing environments known in quantum biological systems.

© 2022 Optica Publishing Group under the terms of the [Optica Open Access Publishing Agreement](#)

1. Introduction

Using quantum coherence and correlations as a resource has become a fundamental topic of research in recent years [1,2]. In quantum metrology, quantum correlations are used to go beyond classical noise measurement limits [3–5]. In quantum thermodynamics, the use of quantum coherence has been proposed to go beyond the Carnot efficiency limit of classical heat engines [6–8]. And in quantum biology, landmark experiments have shown long-lived coherence on the order of hundreds of femtoseconds, suggesting its role in the near-unity energy transfer efficiency of photosynthetic systems [9–11]. The idea of quantum coherence playing a role in photosynthesis is intriguing because it indicates that many-body quantum correlations can exist in ambient conditions with the potential for a wide range of technological applications [12,13].

Energy transfer is typically distinguished as incoherent Förster-type resonance energy transfer (FRET), or coherent excitation energy transfer. The two regimes occur in the limits, $J_{DD}/\gamma_{tot} \ll 1$ and $J_{DD}/\gamma_{tot} \gg 1$, involving the ratio of the electronic dipole-dipole coupling J_{DD} to the total linewidth γ_{tot} of each molecule. The total linewidth is a measure of the coupling strength to the bath's spin, vibrational or electrodynamic degrees of freedom. In photosynthetic systems, the system-bath coupling is primarily dominated by vibrations. The complex nature of photosynthetic systems results in electronic and vibrational coupling strengths varying greatly between the incoherent and coherent coupling limits. Understanding the role of the environment from the weak-to-intermediate-to-strong coupling regimes has been an important topic of interest required to explain experimental observations [14]. In this regard, there has been tremendous progress in the development of a wide variety of open quantum system frameworks (modified-Redfield, Hierarchical equations of motion, Polaron-modified master equation) [15–21] that operate under a wide range of coupling strengths. While a complete understanding of photosynthetic energy transfer has not been achieved [22], there has been a lot of progress outlining how the environment can positively influence energy transfer efficiency [15–21,23–27]. Understanding the role of quantum coherence remains an open problem in photosynthesis, and it is still not clear whether it does play a role [28,29]. It is possible that other guiding principles give rise to near-unity efficiencies in photosynthesis.

Precise control of resonance energy transfer has also emerged as a fundamental topic of interest in the nanophotonic community. There has been a multitude of theoretical [30–34] and experimental [35–41] work proposing and demonstrating nanophotonic control of energy transfer with plasmonic, optical waveguides, and cavity-based systems. Unlike work in the photosynthetic community, most nanophotonic theories of energy transfer have relied on classical electrodynamic descriptions or perturbative approaches based on Fermi’s golden rule. While some authors have provided rigorous quantum electrodynamic formulations, the final analytical expressions are typically valid in either the weak or strong coupling regimes [42–44]. Moreover, a unified definition of efficiency has been lacking in nanophotonics where most results use Förster’s perturbative expression.

In this article, we combine ideas from both communities to develop an exactly solvable theory for resonance energy transfer from first-principles. We derive a quantum master equation providing a unified picture of energy transfer dynamics in the coherent and incoherent coupling regimes applicable in arbitrary Markovian nanophotonic environments. We then solve the model exactly to derive an analytical expression for the energy transfer efficiency. Our result provides insight into the role of finely-tuned coupling strengths, dephasing rates, and detuning between the donor and acceptor required to achieve near-unity energy transfer efficiencies. The central result of this article is the ultimate efficiency of

$$\eta_{max} = \frac{\gamma_a}{\gamma_d + \gamma_a}. \quad (1)$$

This provides a fundamental limit to the energy transfer efficiency between two atoms regardless of coupling strength, quantum coherence and spectral overlap. It also implies the condition $\gamma_a \gg \gamma_d$ is required to achieve near-unity efficiency with the corollary that two identical atoms will have a maximum efficiency of 50%. To the best of our knowledge, this surprisingly simple and intuitive result has not been discussed nor derived in the resonance energy transfer literature. We emphasize this fundamental bound will also apply to quantum transport in the two-chromophore system relevant to many biological systems.

Interestingly, this bound suggests that the acceptor spontaneous emission rate can be used as a new degree of freedom to control energy transfer. To illustrate the interplay of these effects, we predict an experiment to control the efficiency between two atoms above a mirror. We also show that while quantum coherence implies the ultimate efficiency bound has been reached, reaching the ultimate efficiency does not require quantum coherence. Ultimately, these results will enable the design of nanophotonic systems which can mimic quantum biological environments to enhance energy transfer efficiency.

2. Perturbative energy transfer efficiency

We first briefly describe the expression of perturbative energy transfer efficiency for incoherent Förster-type resonance energy transfer. This forms a comparison with the unified nonperturbative definition valid in the weak and strong coupling regimes presented in the next section. The efficiency of Förster resonance energy transfer is conventionally defined as the ratio of the energy transfer rate Γ_{da} to the total dissipation rate of the donor,

$$\eta_{et} = \frac{\Gamma_{da}}{\Gamma_{da} + \gamma_d}. \quad (2)$$

In free-space, the spontaneous emission rate of the donor is $\gamma_d = d_d^2 \omega^3 / (3\pi \hbar \epsilon_0 c^3)$. The energy transfer rate is $\Gamma_{da} = \frac{2\pi}{\hbar^2} |V_{DD}|^2 \mathcal{J}_{da}$ where \mathcal{J}_{da} is the spectral overlap integral of the donor emission and acceptor absorption. The resonant dipole-dipole interaction (RDDI), $V_{DD} = \hbar(-J_{DD} + i\gamma_{DD}/2) = \frac{\omega^2}{\epsilon_0 c^2} \mathbf{d}_a \cdot \mathbf{G}(\mathbf{r}_a, \mathbf{r}_d, \omega) \cdot \mathbf{d}_d$, defines the magnitude of the dipole-dipole coupling. The results are written in terms of the dyadic Green function $\mathbf{G}(\mathbf{r}_a, \mathbf{r}_d, \omega)$

containing both near-field Coulombic and far-field radiative contributions. These definitions of the spontaneous emission and energy transfer rates are based on Fermi's Golden rule valid in the incoherent limit. From these relations, we observe that increasing dipole-dipole coupling ($|V_{DD}| \rightarrow \infty$) results in a near-unity energy transfer efficiency, and therefore no fundamental bound exists for Eq. (2). However, it is worth noting that $J_{DD}/\gamma_{tot} \ll 1$ is required in the weak coupling regime.

3. Non-perturbative energy transfer efficiency

In this article, we follow the extensive work of photosynthetic excitation energy transfer [45,46] and use the following definition for the energy transfer efficiency,

$$\eta_{et} = \gamma_a \int_0^{\infty} \rho_{aa}(t) dt, \quad (3)$$

valid for non-stationary processes such as when the donor is initially in its excited state. This result is general enough to work in the weak and strong coupling regimes between two atoms. Here, the energy transfer efficiency is proportional to the time-integrated luminescence originating from the acceptor. $\rho_{aa}(t)$ is the time-dependent density matrix population of the acceptor in the excited state. More discussions about this definition of energy transfer efficiency can be found in Appendix B. For many applications, this is a much more useful and intuitive definition for energy transfer efficiency.

In Appendix A and Supplement 1, we derive the RDDI master equation for two non-identical atoms of the form, $\frac{\partial}{\partial t} \rho = i[\rho, H_{coh}] + \mathcal{L}[\rho]$, from first principles. The first term involves the coherent dynamics due to dipole-dipole coupling J_{DD} . The second term is a Lindblad superoperator describing the incoherent dynamics due to spontaneous emission and pure dephasing of the donor and acceptor respectively. For the rest of this article, we will ignore non-local cooperative decay γ_{DD} typically associated with superradiant and subradiant effects. We will explore these effects in a future paper. Our results are general enough to work in any Markovian bath with a correlation time τ_c that is much smaller than the relaxation times of the atoms, $\tau_c^{-1} \gg \gamma_d, \gamma_a, \Gamma_{da}$. This extends the range of applicability of this approach beyond the vacuum case, allowing the consideration of more complicated nanophotonic environments. Based on derivations in Appendix B, we obtain the following fundamental relation from the RDDI master equation:

$$\gamma_d \int_0^{\infty} \rho_{dd}(t) dt + \gamma_a \int_0^{\infty} \rho_{aa}(t) dt = 1, \quad (4)$$

where $\rho_{dd}(t)$ is the time-dependent density matrix population of the donor in the excited state. Physically, this equation determines the probability of detecting a single photon from the two-atom system, which must equal one in the long-time limit. Equation (4) can be understood as that, without cooperative decay, this single-photon emission originates from the spontaneous decay of either the acceptor (with probability $\gamma_a \int_0^{\infty} \rho_{aa}(t) dt$) or the donor (with probability $\gamma_d \int_0^{\infty} \rho_{dd}(t) dt$). This result is applicable when a single excitation is initially present in the system. We also assume that both atoms only decay through the emission of a photon, and contributions arising from the cooperative decay are negligible. Equation (4) and the RDDI master equation provide one important insight into the differences between energy transfer efficiency defined in Eq. (2) and Eq. (3). The perturbative definition in Eq. (2) is only valid for irreversible energy transfer from the donor to the acceptor in the weak-coupling limit. In contrast, in Eq. (3), the energy transfer efficiency is defined as the total probability of an acceptor emitting the initial excitation as opposed to the donor. Since the acceptor and donor are treated symmetrically in time evolution governed by the RDDI master equation (with different initial conditions, see Appendix A and B), the definition in Eq. (3) is still valid when reversible energy transfer between acceptor and donor is taken into account in the strong coupling regime.

Using the RDDI master equation, we are able to find the integrated population $\int_0^\infty \rho_{aa}(t) dt$ and simplify Eq. (3) (derivations in Appendix B). A central result of this article is the exact analytical expression of the energy transfer efficiency Eq. (3) valid in the coherent and incoherent coupling regimes,

$$\eta_{et} = \frac{\tilde{\Gamma}_{da}}{\tilde{\Gamma}_{da} + \gamma_d}, \quad (5)$$

where we define the renormalized energy transfer rate,

$$\tilde{\Gamma}_{da} = \frac{\gamma_a \Gamma_{da}}{\gamma_a + \Gamma_{da}}. \quad (6)$$

Surprisingly, we recover the same functional form of Förster's perturbative energy transfer rate, $\Gamma_{da} = \frac{2\pi}{\hbar^2} |V_{DD}|^2 \mathcal{J}_{da}$, however, the master equation approach allows for an exact solution of the spectral overlap integral,

$$\mathcal{J}_{da} = \frac{(\gamma_d + \gamma_{\phi,d} + \gamma_a + \gamma_{\phi,a}) / (2\pi)}{(\tilde{\omega}_d - \tilde{\omega}_a)^2 + (\gamma_d + \gamma_{\phi,d} + \gamma_a + \gamma_{\phi,a})^2 / 4}. \quad (7)$$

The overlap integral \mathcal{J}_{da} is equal to the integral of two Lorentzians with resonant frequencies $\tilde{\omega}_d = \omega_d + \delta\omega_d$, $\tilde{\omega}_a = \omega_a + \delta\omega_a$ and linewidths $\gamma_d + \gamma_{\phi,d}$, $\gamma_a + \gamma_{\phi,a}$ respectively. Here, we introduce $\gamma_{\phi,i}$ as the phenomenological dephasing rate for each atom accounting for fluctuations in the transition frequency. The dephasing rate contributes to an observable linewidth broadening dominant in ambient temperatures where $\gamma_{\phi,i} \gg \gamma_i$.

While the functional form for the energy transfer rate Γ_{da} is similar to conventional FRET theory, this approach goes beyond the perturbative result by taking into account the modification of the resonant frequency and linewidth of each atom, $\delta\omega_i = -\frac{\omega^2}{\hbar\epsilon_0 c^2} \mathbf{d}_i \cdot \text{Re } \mathbf{G}(\mathbf{r}_i, \mathbf{r}_i, \omega) \cdot \mathbf{d}_i$ and $\gamma_i = \frac{2\omega^2}{\hbar\epsilon_0 c^2} \mathbf{d}_i \cdot \text{Im } \mathbf{G}(\mathbf{r}_i, \mathbf{r}_i, \omega) \cdot \mathbf{d}_i$, resulting in modified non-perturbative emission and absorption spectra for the donor and acceptor respectively. In general, the dyadic Green function consists of vacuum and scattered contributions, reinforcing the applicability of this approach to more complicated nanophotonic environments.

4. Maximum energy transfer efficiency

The renormalized energy transfer rate (6) arises from the exact non-stationary solution for two non-identical atoms. The perturbative expression for the FRET efficiency can be recovered when $\Gamma_{da} \ll \gamma_a$. This condition suggests Förster's result is only valid when the acceptor has a fast enough dissipation rate to ensure irreversible energy transfer. In realistic systems, the finite dissipation rate of the acceptor will result in a bottleneck effect. The renormalized energy transfer rate can not exceed the dissipation rate of the acceptor. In the limit of large dipole-dipole coupling, $|V_{DD}| \rightarrow \infty$, the renormalized transfer rate is bounded, $\tilde{\Gamma}_{da} \rightarrow \gamma_a$. The ultimate bound (1) for the energy transfer efficiency immediately follows.

The results for the non-perturbative efficiency η_{et} and the renormalized transfer rate $\tilde{\Gamma}_{da}$ are shown in Fig. 1 for two atoms in vacuum as a function of separation distance. The renormalized transfer rate $\tilde{\Gamma}_{da}$ has a r^{-6} inverse power law dependence until it reaches the bottleneck limit of γ_a , at which point the energy transfer efficiency reaches the fundamental bound. For comparison, we plot the energy transfer efficiency as would be predicted through Förster's expression (black line).

In Fig. 2, we provide numerical evidence of the robustness of this bound to atom-atom detuning $\Delta = \tilde{\omega}_d - \tilde{\omega}_a$ as well as dephasing. It is shown that the fundamental efficiency bound can be approached in the limit of zero detuning, $\Delta \rightarrow 0$. For large detuning, the energy transfer rate will decrease due to poor spectral overlap in the absence of dephasing. As dephasing is increased

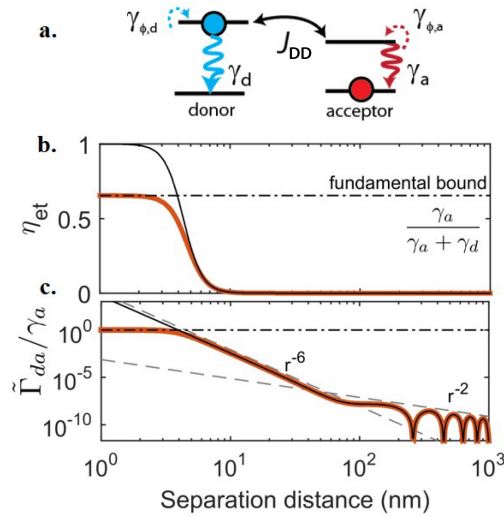


Fig. 1. (a) A donor initially in its excited state will either transfer energy to an acceptor, or spontaneously emit light with rate γ_d . Once the energy is transferred to the acceptor, the energy can either return to the donor or escape into the vacuum with rate γ_a . The energy transfer efficiency is defined as the total probability of an acceptor emitting the initial excitation as opposed to the donor. (b) Using this metric, we find the energy transfer efficiency will have a fundamental bound as the separation distance between two atoms decreases (orange curve), in stark contrast to the conventional definition for the FRET efficiency (black curve). (c) The result can also be understood in terms of the renormalized transfer rate $\tilde{\Gamma}_{da}$ (orange curve) having a fundamental bound as compared to the energy transfer rate Γ_{da} . We take $\gamma_a = 2\gamma_d$ giving an ultimate efficiency of $\eta_{max} = 2/3$.

(see Fig. 2(a)), the energy transfer efficiency reaches a maximum when the following condition is satisfied

$$(\tilde{\omega}_d - \tilde{\omega}_a)^2 = (\gamma_d + \gamma_a + 2\gamma_\phi)^2/4. \tag{8}$$

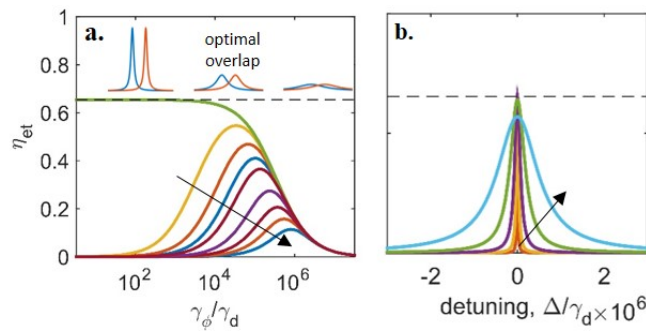


Fig. 2. Energy transfer efficiency as function of (a) dephasing rate γ_ϕ and (b) atom-atom detuning $\Delta = \tilde{\omega}_d - \tilde{\omega}_a$. Note the energy transfer efficiency always remains below the fundamental bound regardless of coupling strengths, spontaneous emission, dephasing or detuning. This bound may be reached asymptotically for the case of two atoms with zero detuning in the limit of small dephasing (green curve left). Black arrow denotes (a) increased detuning and (b) increased dephasing.

Here, we have assumed equal dephasing for both atoms, $\gamma_\phi = \gamma_{\phi,d} = \gamma_{\phi,a}$. Condition (8) corresponds to the optimal emission-absorption spectral overlap. The use of dephasing to enhance efficiency is often referred to as environment assisted quantum transport (ENAQT).

5. Role of quantum coherence

In general, quantum coherence occurs in the strong coupling regime, $|V_{DD}| \gg \gamma_d, \gamma_a, \gamma_\phi$. The strong coupling condition coincides with the condition, $|V_{DD}| \rightarrow \infty$, required to achieve the fundamental bound; therefore, any system with strong coupling and quantum coherence will operate at an efficiency equal to the fundamental bound (1). However, we emphasize the opposite is not true: operating near the fundamental bound does not imply the system has quantum coherence. To demonstrate this effect, we show the population dynamics and efficiency of two distinct systems. We use Woottter's concurrence [47], $C = \max[0, \sqrt{\lambda_1} - \sqrt{\lambda_2} - \sqrt{\lambda_3} - \sqrt{\lambda_4}]$, to measure quantum entanglement. Here, λ_i are the eigenvalues of the operator $\rho(\sigma_y \otimes \sigma_y)\rho^*(\sigma_y \otimes \sigma_y)$ in descending order. A concurrence of 1 implies maximally entangled states while a concurrence of zero implies separable states with zero entanglement. Interestingly, for the non-stationary energy transfer problem the concurrence is exactly equal to the off-diagonal coherence, $C = 2|\rho_{ad}|$, therefore it serves as a measure of both coherence and entanglement. In Fig. 3(a), the system consists of a perfectly tuned donor-acceptor pair, $\Delta = 0$, with zero dephasing. This system achieves the ultimate efficiency of $\eta_{max} = 2/3$. The time-dependent concurrence (bottom plot) clearly shows quantum coherence is present in this system. In Fig. 3(b), we have two detuned atoms $\Delta/(2\pi) = 10$ THz with large dephasing $\gamma_\phi/(2\pi) = 4$ THz close to the necessary condition (8) for optimal spectral overlap. Interestingly, the second system exhibits irreversible energy transfer with negligible concurrence and therefore lacks quantum coherence but nevertheless reaches an efficiency that lies within 1 percent of the fundamental bound. The clear advantage of quantum coherence is that it reaches η_{max} for longer distances, $r = 45$ nm, while the detuned system requires a separation distance of $r = 4.5$ nm.

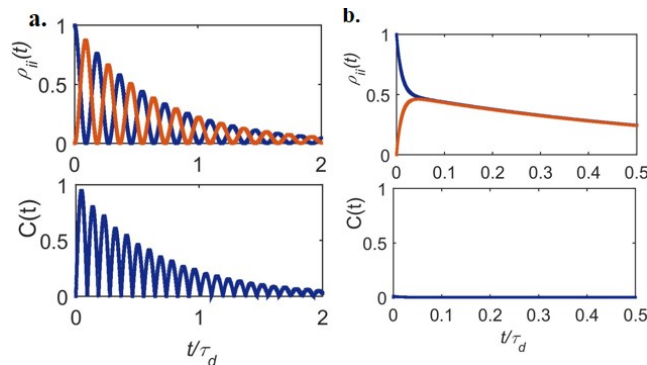


Fig. 3. Population dynamics of donor (blue) and acceptor (orange) as well as concurrence (bottom) used as a measure of quantum coherence. (a) Quantum coherent energy transfer between two atoms ($r = 45$ nm) operating at the ultimate efficiency $\eta_{max} = 2/3$. (b) Irreversible energy transfer between two atoms ($r = 4.5$ nm) operating within 1 percent of the ultimate efficiency exhibiting negligible quantum coherence.

6. Nanophotonic control of energy transfer efficiency

The fundamental bound (1) suggests a new design strategy for increasing the energy transfer efficiency based on the control of donor and acceptor spontaneous emission rates. In Fig. 4, we present a canonical example illustrating how a nanophotonic environment can positively

influence the energy transfer efficiency between two atoms using a non-resonant silver mirror eliminating the need for high-Q cavities. Here, we consider donor and acceptor with spontaneous emission rates in vacuum $\gamma_{0,a} = 2\gamma_{0,d} = 4\pi$ GHz, transition frequencies $\omega_a/(2\pi) = 545$ THz and $\omega_d/(2\pi) = 550$ THz, and dephasing rates $\gamma_{\phi,a} = \gamma_{\phi,d} = 4\pi$ THz. A Drude model with the plasma frequency $\omega_p/(2\pi) = 2000$ THz and the damping factor $\lambda = 0.005 \omega_p$ is used for the dielectric properties of the silver mirror. The basic idea is to use an orientation-dependent Purcell effect close to the mirror, understood through an image dipole model (inset). A parallel dipole close to a mirror will form an image dipole with the opposite orientation suppressing spontaneous emission, while a perpendicular dipole close to a mirror will form a collinear image dipole enhancing spontaneous emission. This suggests an ideal configuration where the donor is parallel and the acceptor is perpendicular to the mirror surface (orange curve). The mirror-enhanced efficiency bound only depends on spontaneous emission rates of the donor and acceptor and can be reached at approximately 10 nm from the mirror. Note that this configuration is typically forbidden in free-space, but becomes possible due to image dipole formation.

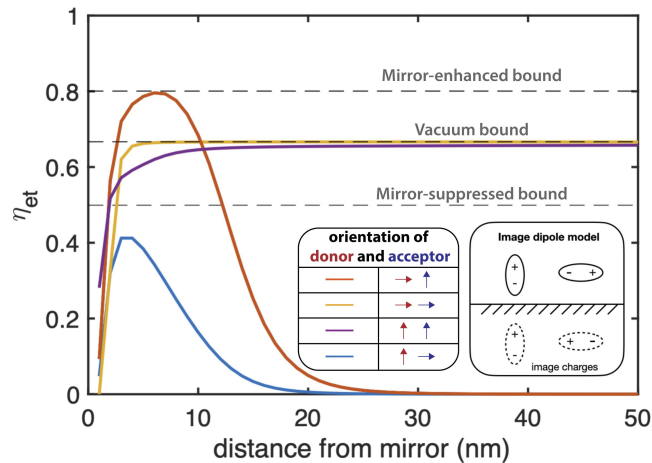


Fig. 4. Nanophotonic control of energy transfer between two atoms above a silver mirror. Here, we provide an example of how the environment can positively or negatively influence the energy transfer efficiency based primarily on the transition dipole moment orientation. We consider two atoms with spontaneous emission rates $\gamma_a = 2\gamma_d$ corresponding to a vacuum bound of $\eta_{max} = 2/3$. To overcome the vacuum bound, we propose using the orientation dipole moments of each atom relative to the mirror to control spontaneous emission rates. The ideal configuration corresponds to a donor parallel to a mirror and an acceptor perpendicular to a mirror, as it achieves the condition $\gamma_a \gg \gamma_d$ around 10 nm from the mirror. In this scenario, the environment modifies the fundamental bound of the energy transfer efficiency resulting in an overall enhancement. The opposite configuration (blue) will decrease the fundamental bound, suppressing the overall energy transfer efficiency. Results are calculated with the full dyadic Green function for two atoms $r = 10$ nm apart.

7. Conclusion

To conclude, we derive a fundamental efficiency bound for resonance energy transfer between two atoms arising in the limit of large dipole-dipole coupling. We use the bound to derive design principles for controlling energy transfer in nanophotonics and present an exactly solvable canonical example to illustrate the interplay of these effects. We emphasize this bound ignores the role of the cooperative decay rate γ_{DD} ; therefore, future work should focus on its role in altering the efficiency of energy transfer. Our results pave the way towards a critical understanding of

the role of the environment in resonance energy transfer using nanophotonic and metamaterial approaches [48–50]. Future work will focus on developing a rigorous non-Markovian theory (e.g., see [51]) of energy transfer with wider applicability.

Appendix A: Quantum electrodynamic theory of energy transfer

We use a quantum electrodynamic (QED) theory to describe the interaction between two neutral atoms in an arbitrary nanophotonic environment. In the dipole approximation, the multipolar Hamiltonian is composed of three components, $H = H_s + H_b + H_{int}$, where

$$\begin{aligned} H_s &= \sum_{n=g,e} \hbar\omega_{n,d} |n_d\rangle\langle n_d| + \sum_{n=g,e} \hbar\omega_{n,a} |n_a\rangle\langle n_a|, \\ H_b &= \int d^3\mathbf{r} \int_0^\infty d\omega \hbar\omega \hat{\mathbf{f}}^\dagger(\mathbf{r}, \omega) \hat{\mathbf{f}}(\mathbf{r}, \omega), \\ H_{int} &= -\hat{\mathbf{d}}_d \cdot \hat{\mathbf{E}}(\mathbf{r}_d) - \hat{\mathbf{d}}_a \cdot \hat{\mathbf{E}}(\mathbf{r}_a), \end{aligned} \quad (9)$$

H_s describes the two-atom system, H_b the electrodynamic bath, and H_{int} the electric-dipole interaction between each atom's electric dipole moment $\hat{\mathbf{d}}_k = \hat{\mathbf{d}}_{eg}^k \sigma_k^+ + \hat{\mathbf{d}}_{ge}^k \sigma_k^-$ and the electrodynamic field respectively, $k = \{d, a\}$. We assume each atom only has two electronic energy levels while also ignoring multipolar and spin contributions. This Hamiltonian has been derived previously by several authors and forms the basis of an *effective-field/macroscopic* quantum electrodynamic theory valid in arbitrary dissipative media satisfying Kramers-Kronig causality relations [44,52]. Here, $\hat{\mathbf{f}}^\dagger(\mathbf{r}, \omega)/\hat{\mathbf{f}}(\mathbf{r}, \omega)$ represent the creation/annihilation operators of the elementary excitations of matter. In vacuum, $\hat{\mathbf{f}}^\dagger(\mathbf{r}, \omega)$ describes the creation of a *photon*. In macroscopic matter, it describes the creation of a *polariton*. These operators satisfy

$$\hat{\mathbf{f}}(\mathbf{r}, \omega)|\{0\}\rangle = 0 \quad \text{and} \quad \hat{\mathbf{f}}^\dagger(\mathbf{r}, \omega)|\{0\}\rangle = |\mathbf{1}(\mathbf{r}, \omega)\rangle,$$

as well as

$$[\hat{\mathbf{f}}(\mathbf{r}, \omega), \hat{\mathbf{f}}^\dagger(\mathbf{r}', \omega')] = \delta(\mathbf{r} - \mathbf{r}')\delta(\omega - \omega') \quad \text{and} \quad [\hat{\mathbf{f}}(\mathbf{r}, \omega), \hat{\mathbf{f}}(\mathbf{r}', \omega')] = 0.$$

In dissipative quantum electrodynamics, the electric field is defined as

$$\hat{\mathbf{E}}(\mathbf{r}, \omega) = i\sqrt{\frac{\hbar\omega^4}{\pi\epsilon_0 c^4}} \int d^3\mathbf{r}' \sqrt{\epsilon(\mathbf{r}', \omega)} \mathbf{G}(\mathbf{r}, \mathbf{r}', \omega) \hat{\mathbf{f}}(\mathbf{r}', \omega), \quad (10)$$

written in terms the imaginary part of the inhomogeneous and frequency dependent permittivity, $\epsilon(\mathbf{r}, \omega) = \epsilon'(\mathbf{r}, \omega) + i\epsilon''(\mathbf{r}, \omega)$, as well as the classical dyadic Green function $\mathbf{G}(\mathbf{r}, \mathbf{r}', \omega)$. We provide exact expressions for the Green function in Appendix D. The electric field is decomposed in terms of positive-frequency and negative-frequency components, $\hat{\mathbf{E}}(\mathbf{r}) = \hat{\mathbf{E}}^{(+)}(\mathbf{r}) + \hat{\mathbf{E}}^{(-)}(\mathbf{r})$, where $\hat{\mathbf{E}}^{(+)}(\mathbf{r}) = \int_0^\infty d\omega \hat{\mathbf{E}}(\mathbf{r}, \omega)$, while also satisfying the condition $[\hat{\mathbf{E}}^{(-)}(\mathbf{r})]^\dagger = \hat{\mathbf{E}}^{(+)}(\mathbf{r})$. In the following, we derive the quantum master equation describing the atom-atom dynamics arising from the Hamiltonian Eq. (9). While such a master equation has been derived before, it is worth re-visiting the derivation to account for inconsistencies between different models. We will discuss this subtle point later on. To obtain a closed-form solution without the use of the rotating wave approximation, we truncate the Hilbert space to the following states,

$$|d\rangle \equiv |e_d, g_a, \{0\}\rangle, \quad |a\rangle \equiv |g_d, e_a, \{0\}\rangle, \quad |g\rangle \equiv |g_d, g_a, \mathbf{1}(\mathbf{r}, \omega)\rangle, \quad |e\rangle \equiv |e_d, e_a, \mathbf{1}(\mathbf{r}, \omega)\rangle,$$

corresponding to an excited-state donor with acceptor and field in the ground-state, an excited-state acceptor with donor and field in ground-state, a single-excitation in the field with both atoms in

the ground state, and finally a single field excitation with both atoms in the excited-state. Due to truncation of the Hilbert space, this approach is not fully non-perturbative and will fail to describe higher-order multi-photon effects that occur in the ultra-strong coupling regime. In the truncated Hilbert space, the temporal evolution of the system is captured by the total wavefunction

$$|\psi(t)\rangle = d(t)|d\rangle + a(t)|a\rangle + \int d^3\mathbf{r} \int d\omega g(\mathbf{r}, \omega, t)|g\rangle + \int d^3\mathbf{r} \int d\omega e(\mathbf{r}, \omega, t)|e\rangle. \quad (11)$$

Using the Schrodinger equation, $i\hbar \frac{\partial}{\partial t} |\psi(t)\rangle = H|\psi(t)\rangle$, we obtain the dynamical equations for the probability amplitudes,

$$i\hbar \frac{\partial d}{\partial t} = \hbar(\omega_{g,a} + \omega_{e,d})d(t) + \int d^3\mathbf{r} \int d\omega [g(\mathbf{r}, \omega, t)V_{dg} + e(\mathbf{r}, \omega, t)V_{de}], \quad (12)$$

$$i\hbar \frac{\partial a}{\partial t} = \hbar(\omega_{g,d} + \omega_{e,a})a(t) + \int d^3\mathbf{r} \int d\omega [g(\mathbf{r}, \omega, t)V_{ag} + e(\mathbf{r}, \omega, t)V_{ae}], \quad (13)$$

$$i\hbar \frac{\partial g}{\partial t} = \hbar(\omega_{g,a} + \omega_{g,d} + \omega')g(\mathbf{r}', \omega', t) + V_{gd}d(t) + V_{ga}a(t), \quad (14)$$

$$i\hbar \frac{\partial e}{\partial t} = \hbar(\omega_{e,a} + \omega_{e,d} + \omega')e(\mathbf{r}', \omega', t) + V_{ed}d(t) + V_{ea}a(t), \quad (15)$$

where we define $V_{kn} = \langle k|H_{int}|n(\mathbf{r}, \omega)\rangle$ as the interaction coupling coefficient with $k = \{a, d\}$ and $n = \{g, e\}$. In the following, we present the exact analytical response for the case of two atoms in a *Markovian* nanophotonic environment.

Probability amplitude equations of motion. In [Supplement 1](#), we provide the detailed derivation of obtaining probability amplitude equations of motion for $d(t)$ and $a(t)$ from Eq. (12)–(15). After simplifying the equations with properties of creation and annihilation operators and employing Markov approximation, we obtain the following set of coupled differential equations for the probability amplitudes in the Schrodinger picture,

$$i\hbar \frac{\partial d}{\partial t} = -[\tilde{\Sigma}_{e,d} + \tilde{\Sigma}_{g,a}]d(t) - V_{da}a(t), \quad (16)$$

$$i\hbar \frac{\partial a}{\partial t} = -V_{ad}d(t) - [\tilde{\Sigma}_{g,d} + \tilde{\Sigma}_{e,a}]a(t). \quad (17)$$

We have written everything in terms of a modified excited-state self-energy $\tilde{\Sigma}_{e,k} = -\hbar\omega_{e,k} + \Sigma_{e,k}$, modified ground-state self-energy $\tilde{\Sigma}_{g,k} = -\hbar\omega_{g,k} + \Sigma_{g,k}$, and resonant dipole-dipole interaction (RDDI) $V_{kk'} = \hbar(-J_{kk'} + i\gamma_{kk'}/2)$, taking into account the bare transition frequencies of both atoms ($k, k' = \{a, d\}$). The excited-state self-energy is $\Sigma_{e,k} = \hbar(-\delta\omega_{e,k} + i\gamma_k/2)$, where

$$\delta\omega_{e,k} = \frac{\mathcal{P}}{\hbar\epsilon_0\pi} \int_0^\infty d\omega \frac{\omega^2 \mathbf{d}_{eg}^k \cdot \text{Im}\mathbf{G}(\mathbf{r}_k, \mathbf{r}_k, \omega) \cdot \mathbf{d}_{ge}^k}{c^2 (\omega_k - \omega)}, \quad (18)$$

$$\gamma_k = \frac{2\omega_k^2}{\hbar\epsilon_0 c^2} \mathbf{d}_{eg}^k \cdot \text{Im}\mathbf{G}(\mathbf{r}_k, \mathbf{r}_k, \omega_k) \cdot \mathbf{d}_{ge}^k. \quad (19)$$

The ground-state self-energy is $\Sigma_{g,k} = -\hbar\delta\omega_{g,k}$, where

$$\delta\omega_{g,k} = -\frac{\mathcal{P}}{\hbar\epsilon_0\pi} \int_0^\infty d\omega \frac{\omega^2 \mathbf{d}_{ge}^k \cdot \text{Im}\mathbf{G}(\mathbf{r}_k, \mathbf{r}_k, \omega) \cdot \mathbf{d}_{eg}^k}{c^2 (\omega_k + \omega)}. \quad (20)$$

The resonant dipole-dipole interaction (RDDI) $V_{kk'}$ is

$$\gamma_{kk'} = \frac{2\omega_+^2}{\hbar\epsilon_0 c^2} \mathbf{d}_{eg}^k \cdot \text{Im}\mathbf{G}(\mathbf{r}_k, \mathbf{r}_{k'}, \omega_+) \cdot \mathbf{d}_{ge}^{k'}, \quad (21)$$

$$J_{kk'} = -\frac{\omega_+^2}{\hbar\epsilon_0 c^2} \mathbf{d}_{eg}^k \cdot \text{Re} \mathbf{G}(\mathbf{r}_k, \mathbf{r}_{k'}, \omega_+) \cdot \mathbf{d}_{ge}^{k'}, \quad (22)$$

$$V_{kk'} = \hbar(-J_{kk'} + i\gamma_{kk'}/2) = \frac{\omega_+^2}{\epsilon_0 c^2} \mathbf{d}_{eg}^k \cdot \mathbf{G}(\mathbf{r}_k, \mathbf{r}_{k'}, \omega_+) \cdot \mathbf{d}_{ge}^{k'}. \quad (23)$$

Detailed derivations of Eq. (18)–(23) can be found in [Supplement 1](#). These coupled differential equations form the main result of this sub-section.

RDDI quantum master equation. Using (16), (17), we find the following set of coupled differential equations for the populations and coherences,

$$\frac{\partial}{\partial t} |d|^2 = \frac{2}{\hbar} \text{Re} [i(\tilde{\Sigma}_{e,d} + \tilde{\Sigma}_{g,a})|d|^2 + iV_{da}da^*], \quad (24)$$

$$\frac{\partial}{\partial t} |a|^2 = \frac{2}{\hbar} \text{Re} [iV_{ad}da^* + i(\tilde{\Sigma}_{g,d} + \tilde{\Sigma}_{e,a})|a|^2], \quad (25)$$

$$\frac{\partial}{\partial t} (da^*) = \frac{1}{i\hbar} [-\tilde{\Sigma}_{e,d} + \tilde{\Sigma}_{g,a}]da^* - V_{da}|a|^2 + V_{ad}|d|^2 + (\tilde{\Sigma}_{g,d} + \tilde{\Sigma}_{e,a})^* da^*. \quad (26)$$

Using the definition of the density matrix $\rho = |\phi\rangle\langle\phi|$, it is straightforward to show that these equations are equivalent to the RDDI quantum master equation,

$$\frac{\partial}{\partial t} \rho = -\frac{i}{\hbar} [H_{coh}, \rho] - \sum_{k,k'} \frac{\gamma_{kk'}}{2} [\sigma_k^\dagger \sigma_{k'} \rho - 2\sigma_{k'} \rho \sigma_k^\dagger + \rho \sigma_k^\dagger \sigma_{k'}], \quad (27)$$

where the first term contains the coherent Hamiltonian, $H_{coh} = \sum_{n=g,e} (\omega_{n,d} + \delta\omega_{n,d}) \sigma_d^\dagger \sigma_d + \sum_{n=g,e} (\omega_{n,a} + \delta\omega_{n,a}) \sigma_a^\dagger \sigma_a + \sum_{k \neq k'} J_{kk'} \sigma_k^\dagger \sigma_{k'}$, while the second term contains the relevant dissipative terms. The RDDI master equation has been derived here for two non-identical atoms. We emphasize this equation describes coherent coupling between two atoms in a Markovian reservoir but cannot describe non-Markovian dynamics or multi-photon effects arising from strong-coupling between the atoms and the electrodynamic bath. In other words, it must operate in a regime where the frequency shifts and dipole-dipole couplings are much smaller than the transition frequencies of the atoms ($\delta\omega_k, J_{kk'} \ll \omega_k, \omega_{k'}$). Going beyond this regime requires an expansion of the Hilbert space and corresponds to the ultra-strong coupling regime. To recover the semi-classical Förster regime, we must include a phenomenological dephasing term for each atom described by the super-operators, $\gamma_{\phi,d} \mathcal{L}_{\phi,d} + \gamma_{\phi,a} \mathcal{L}_{\phi,a}$. These terms describe fluctuations in the energy levels resulting in linewidth broadening and loss of coherence. Explicitly, the dephasing super-operators acting on the density operator in the single-excitation, excited-state sub-space are

$$\mathcal{L}_{\phi,d} = \mathcal{L}[\hat{\sigma}_d^\dagger \hat{\sigma}_d] \rho = -\frac{1}{2} \begin{pmatrix} 0 & \rho_{da} \\ \rho_{ad} & 0 \end{pmatrix}, \quad \mathcal{L}_{\phi,a} = \mathcal{L}[\hat{\sigma}_a^\dagger \hat{\sigma}_a] \rho = -\frac{1}{2} \begin{pmatrix} 0 & \rho_{da} \\ \rho_{ad} & 0 \end{pmatrix}.$$

Combining the results above, we find the single-excitation populations satisfy

$$\dot{\rho}_{dd} = \frac{i}{\hbar} (V_{da}\rho_{ad} - V_{da}^*\rho_{da}) - \gamma_d \rho_{dd}, \quad (28)$$

$$\dot{\rho}_{aa} = \frac{i}{\hbar} (V_{ad}\rho_{da} - V_{ad}^*\rho_{ad}) - \gamma_a \rho_{aa}, \quad (29)$$

while the coherences obey

$$\dot{\rho}_{da} = +i\omega_1 \rho_{da} + \frac{i}{\hbar} (V_{da}\rho_{aa} - V_{ad}^*\rho_{dd}), \quad (30)$$

$$\dot{\rho}_{ad} = -i\omega_1^* \rho_{ad} - \frac{i}{\hbar} (V_{da}^* \rho_{aa} - V_{ad} \rho_{dd}). \quad (31)$$

To simplify the equations, we defined $\omega_1 = \Delta_1 + i\gamma_1$, with $\Delta_1 = (\tilde{\omega}_a - \tilde{\omega}_d)$ and $\gamma_1 = (\gamma_d + \gamma_{\phi,d} + \gamma_a + \gamma_{\phi,a})/2$. We have also defined $\tilde{\omega}_a = \omega_a + \delta\omega_a = (\omega_{e,a} - \omega_{g,a}) + (\delta\omega_{e,a} - \delta\omega_{g,a})$, and $\tilde{\omega}_d = \omega_d + \delta\omega_d = (\omega_{e,d} - \omega_{g,d}) + (\delta\omega_{e,d} - \delta\omega_{g,d})$ for notational simplicity.

Appendix B: Non-stationary energy transfer efficiency

In this section, we derive the fundamental relation that provides a unified treatment of the energy transfer efficiency in the coherent and incoherent coupling regimes. The non-stationary energy transfer efficiency is obtained by integrating the population Eqs. (28), (29) from 0 to ∞ ,

$$\rho_{dd}(\infty) - \rho_{dd}(0) = -1 = \frac{i}{\hbar} V_{da} \int_0^\infty \rho_{ad}(t) dt - \frac{i}{\hbar} V_{da}^* \int_0^\infty \rho_{da}(t) dt - \gamma_d \int_0^\infty \rho_{dd}(t) dt, \quad (32)$$

$$\rho_{aa}(\infty) - \rho_{aa}(0) = 0 = \frac{i}{\hbar} V_{ad} \int_0^\infty \rho_{da}(t) dt - \frac{i}{\hbar} V_{ad}^* \int_0^\infty \rho_{ad}(t) dt - \gamma_a \int_0^\infty \rho_{aa}(t) dt. \quad (33)$$

We have assumed the donor is initially in the excited state, $\rho_{dd}(0) = 1$, with the acceptor in the ground state, $\rho_{aa}(0) = 0$. In the long-time limit, the initial excitation leaves the donor-acceptor system resulting in $\rho_{dd}(\infty) = \rho_{aa}(\infty) = 0$. As adding the population Eqs. (32), (33) yields the fundamental relation (note that when the cooperative decay is neglected, V_{da} and V_{ad} are real) Eq. (4). Physically, this equation determines the probability of detecting a single photon from the two-atom system, which must equal one in the long-time limit. This result is applicable when a single excitation is initially present in the system. We also assume that both atoms have unit quantum efficiency and only decay through the emission of a photon. We emphasize this result is based on the assumption that contributions arising from the cooperative decay are negligible, i.e. $\gamma_{da} = 0$. Neglecting the cooperative decay rate recovers many of the photosynthetic energy transfer models used in the literature. We will discuss this assumption more thoroughly in a future manuscript. From Ref. [45], the energy transfer efficiency is defined as Eq. (3), which is valid in both the coherent and incoherent coupling limits.

Exact solution to the energy transfer efficiency. There are two approaches to finding the integrated population $\int_0^\infty \rho_{aa}(t') dt'$. The first approach finds the expression for $\rho_{aa}(t')$, then performs the time integral analytically. We introduce a second approach here. Integrating the coherence differential equations, (30), (31), from 0 to ∞ , we substitute the result into (32), (33),

$$-1 = -(\tilde{\gamma}_d + \Gamma_{da}) \bar{\rho}_{dd} + \Gamma_{da} \bar{\rho}_{aa}, \quad (34)$$

$$0 = -(\tilde{\gamma}_a + \Gamma_{da}) \bar{\rho}_{aa} + \Gamma_{da} \bar{\rho}_{dd}, \quad (35)$$

where we have defined $\bar{\rho}_{kk} = \int_0^\infty \rho_{kk}(t') dt'$ for the donor and acceptor respectively $k = \{d, a\}$. We also introduce the bare energy transfer rate,

$$\Gamma_{da} = \frac{|V_{DD}|^2}{\hbar^2} \frac{(\gamma_d + \gamma_{\phi,d} + \gamma_a + \gamma_{\phi,a})}{(\tilde{\omega}_d - \tilde{\omega}_a)^2 + (\gamma_d + \gamma_{\phi,d} + \gamma_a + \gamma_{\phi,a})^2/4}, \quad (36)$$

where $|V_{DD}|^2 = |V_{da}|^2$. Solving for $\bar{\rho}_{aa}$, the non-perturbative expression for the efficiency is

$$\eta = \frac{\tilde{\Gamma}_{da}}{\tilde{\Gamma}_{da} + \gamma_d}, \quad (37)$$

where $\tilde{\Gamma}_{da}$ is the *renormalized* energy transfer rate

$$\tilde{\Gamma}_{da} = \frac{\gamma_a \Gamma_{da}}{\gamma_a + \Gamma_{da}}, \quad (38)$$

as shown in the main paper. This modified energy transfer rate is one of the major results of the paper highlighting the drastic modification of the energy transfer efficiency compared to previous

theoretical models. These results imply a fundamental bound for the energy transfer rate and efficiency as discussed in the main manuscript. Note we have also derived the same analytical expression using the first approach, i.e. analytically evaluating the time-integral.

Appendix C: Quantum correlations in energy transfer

In the following, we introduce Wooteer's definition of concurrence [47] to describe quantum entanglement between two qubits.

Concurrence. The general wavefunction describing 2 qubits is

$$|\psi\rangle = \alpha|e_d, e_a\rangle + \beta|e_d, g_a\rangle + \gamma|g_d, e_a\rangle + \delta|g_d, g_a\rangle. \quad (39)$$

An appropriate measure of entanglement, given by the concurrence, is $C = 2|\alpha\delta - \gamma\beta| \geq 0$. A concurrence of 1 refers to a maximally-entangled state, while $C = 0$ refers to separable states. In the energy transfer problem with a single excitation ($\alpha = 0$), the concurrence is simply given by $C = 2|\beta\gamma|$. Using the notation of section 1, the time-dependent concurrence is $C(t) = 2|d(t)a(t)|$. The result is easily generalized for a density operator describing mixed states. Here, the concurrence is defined as

$$C = \max[0, \sqrt{\lambda_1} - \sqrt{\lambda_2} - \sqrt{\lambda_3} - \sqrt{\lambda_4}], \quad (40)$$

where λ_i are the eigenvalues of the operator $\rho(\sigma_y \otimes \sigma_y)\rho^*(\sigma_y \otimes \sigma_y)$ in descending order. For the non-stationary energy transfer problem where the donor is initially in the excited-state, the eigenvalues are readily solved analytically giving the final result

$$C = 2|\rho_{da}|, \quad (41)$$

and is therefore exactly dependent on the coherence between both atoms in the site basis. Concurrence provides a measure of entanglement as well as coherence, making it an appropriate choice for studying non-classicality in the energy transfer problem.

Appendix D: Two atoms above a mirror

Free-space Green function. Here, we provide the full Green function expression for two atoms above a mirror. The dyadic Green function in a bulk medium with refractive index $n = \sqrt{\epsilon}$ satisfies the vector wave equation,

$$\nabla \times \nabla \times \mathbf{G}_o(\mathbf{r}, \mathbf{r}'; \omega) - \epsilon \frac{\omega^2}{c^2} \mathbf{G}_o(\mathbf{r}, \mathbf{r}'; \omega) = \mathbf{1} \delta(\mathbf{r} - \mathbf{r}'). \quad (42)$$

The homogeneous Green function has a well-known solution ($k = \sqrt{\epsilon} \omega/c$):

$$\mathbf{G}_o(\mathbf{r}) = \left[\frac{1}{k^2} \nabla \otimes \nabla + \mathbf{I} \right] \frac{e^{ikr}}{4\pi r} \quad (43)$$

$$= \frac{e^{ikr}}{4\pi k^2 r^3} \left[(k^2 r^2 + ikr - 1) \mathbf{I} + (3 - 3ikr - k^2 r^2) \hat{\mathbf{r}} \otimes \hat{\mathbf{r}} \right] - \frac{1}{3k^2} \delta(\mathbf{r}) \mathbf{I}, \quad (44)$$

containing both Coulombic near-field ($kr \ll 1$) and radiative far-field ($kr \gg 1$) components. We use this result for plotting Fig. 1.

Scattered Green function. In the following, we provide the scattered Green function for two atoms above a mirror defined through the normal unit vector $\mathbf{n} = \hat{\mathbf{e}}_z$. The scattered Green function is found self-consistently through the use of electrodynamic boundary conditions. It is

possible to show, upon simplification, that the scattered Green function takes the following form in cylindrical coordinates [43]

$$G_{xx}^s(\mathbf{r}) = \frac{i}{8\pi k^2} \int dk_\rho \frac{k_\rho}{k_z} e^{2ik_z d} [k_1^2 J_+ r_s - k_z^2 J_- r_p], \quad (45)$$

$$G_{xz}^s(\mathbf{r}) = \frac{i}{8\pi k^2} \int dk_\rho \frac{k_\rho}{k_z} e^{2ik_z d} [-2ik_\rho k_z J_1(k_\rho \rho) r_p], \quad (46)$$

$$G_{zx}^s(\mathbf{r}) = \frac{i}{8\pi k^2} \int dk_\rho \frac{k_\rho}{k_z} e^{2ik_z d} [+2ik_\rho k_z J_1(k_\rho \rho) r_p], \quad (47)$$

$$G_{zz}^s(\mathbf{r}) = \frac{i}{8\pi k^2} \int dk_\rho \frac{k_\rho}{k_z} e^{2ik_z d} [2k_\rho^2 J_0(k_\rho \rho) r_p], \quad (48)$$

where d is the distance of the donor and acceptor from the mirror interface, and ρ is the lateral separation distance between the donor and acceptor. We also introduced $J_\pm = J_0(k_\rho \rho) \pm J_2(k_\rho \rho)$, where $J_n(k_\rho \rho)$ is the cylindrical Bessel function of order n . The Fresnel reflection coefficients for p and s polarized light are:

$$r_p = \frac{\epsilon_2 k_z - \epsilon k_{z2}}{\epsilon_2 k_z + \epsilon k_{z2}} \quad \text{and} \quad r_s = \frac{k_z - k_{z2}}{k_z + k_{z2}}, \quad (49)$$

with z -component wavevectors, $k_z = \sqrt{\epsilon \omega^2 / c^2 - k_\rho^2}$ and $k_{z2} = \sqrt{\epsilon_2 \omega^2 / c^2 - k_\rho^2}$. The full Green function integral is evaluated numerically using an adaptive Gauss-Kronrod quadrature. A Drude model with the plasma frequency $\omega_p / (2\pi) = 2000$ THz and the damping factor $\lambda = 0.005 \omega_p$ has been used for the dielectric properties of the silver mirror.

Funding. Defense Advanced Research Projects Agency (N66001-17-1-4048).

Disclosures. The authors declare no conflicts of interest.

Data availability. Data underlying the results presented in this paper are not publicly available at this time but may be obtained from the authors upon reasonable request.

Supplemental document. See [Supplement 1](#) for supporting content.

References

1. G. Adesso, T. R. Bromley, and M. Cianciaruso, "Measures and applications of quantum correlations," *J. Phys. A: Math. Theor.* **49**(47), 473001 (2016).
2. A. Streltsov, G. Adesso, and M. B. Plenio, "Colloquium: Quantum coherence as a resource," *Rev. Mod. Phys.* **89**(4), 041003 (2017).
3. S. Lloyd, "Enhanced sensitivity of photodetection via quantum illumination," *Science* **321**(5895), 1463–1465 (2008).
4. G. Brida, I. P. Degiovanni, M. Genovese, E. D. Lopaeva, A. Meda, and I. R. Berchera, "Beyond classical limits by exploiting quantum light: a short review of inrim results," *J. Phys.: Conf. Ser.* **442**, 012022 (2013).
5. I. Bechera, A. Meda, I. Degiovanni, and G. Brida, "Overcoming classical measurement limits through photon number correlations: An overview of a few recent results," *Proc. SPIE* **9225**, 922502 (2014).
6. M. O. Scully, M. S. Zubairy, G. S. Agarwal, and H. Walther, "Extracting work from a single heat bath via vanishing quantum coherence," *Science* **299**(5608), 862–864 (2003).
7. K. E. Dorfman, D. V. Voronine, S. Mukamel, and M. O. Scully, "Photosynthetic reaction center as a quantum heat engine," *Proc. Natl. Acad. Sci.* **110**(8), 2746–2751 (2013).
8. J. Roßnagel, O. Abah, F. Schmidt-Kaler, K. Singer, and E. Lutz, "Nanoscale heat engine beyond the carnot limit," *Phys. Rev. Lett.* **112**(3), 030602 (2014).
9. G. S. Engel, T. R. Calhoun, E. L. Read, T.-K. Ahn, T. Mančal, Y.-C. Cheng, R. E. Blankenship, and G. R. Fleming, "Evidence for wavelike energy transfer through quantum coherence in photosynthetic systems," *Nature* **446**(7137), 782–786 (2007).
10. E. Collini, C. Y. Wong, K. E. Wilk, P. M. Curmi, P. Brumer, and G. D. Scholes, "Coherently wired light-harvesting in photosynthetic marine algae at ambient temperature," *Nature* **463**(7281), 644–647 (2010).
11. G. Panitchayangkoon, D. Hayes, K. A. Fransted, J. R. Caram, E. Harel, J. Wen, R. E. Blankenship, and G. S. Engel, "Long-lived quantum coherence in photosynthetic complexes at physiological temperature," *Proc. Natl. Acad. Sci.* **107**(29), 12766–12770 (2010).

12. E. Romero, R. Augulis, V. I. Novoderezhkin, M. Ferretti, J. Thieme, D. Zigmantas, and R. Van Grondelle, "Quantum coherence in photosynthesis for efficient solar energy conversion," *Nat. Phys.* **10**(9), 676–682 (2014).
13. J.-L. Brédas, E. H. Sargent, and G. D. Scholes, "Photovoltaic concepts inspired by coherence effects in photosynthetic systems," *Nat. Mater.* **16**(1), 35–44 (2017).
14. A. Chenu and G. D. Scholes, "Coherence in energy transfer and photosynthesis," *Annu. Rev. Phys. Chem.* **66**(1), 69–96 (2015).
15. M. Yang and G. R. Fleming, "Influence of phonons on exciton transfer dynamics: comparison of the Redfield, Förster, and modified Redfield equations," *Chem. Phys.* **275**(1-3), 355–372 (2002).
16. A. Ishizaki and G. R. Fleming, "Unified treatment of quantum coherent and incoherent hopping dynamics in electronic energy transfer: Reduced hierarchy equation approach," *The Journal of Chemical Physics* **130**(23), 234111 (2009).
17. C. Wang, J. Ren, and J. Cao, "Nonequilibrium energy transfer at nanoscale: A unified theory from weak to strong coupling," *Sci. Rep.* **5**(1), 11787 (2015).
18. D. Beljonne, C. Curutchet, G. D. Scholes, and R. J. Silbey, "Beyond forster resonance energy transfer in biological and nanoscale systems," *The Journal of Physical Chemistry B* **113**(19), 6583–6599 (2009).
19. Y. Tanimura, "Reduced hierarchical equations of motion in real and imaginary time: Correlated initial states and thermodynamic quantities," *The Journal of Chemical Physics* **141**(4), 044114 (2014).
20. E. N. Zimanyi and R. J. Silbey, "Theoretical description of quantum effects in multi-chromophoric aggregates," *Phil. Trans. R. Soc. A.* **370**(1972), 3620–3637 (2012).
21. D. P. McCutcheon and A. Nazir, "Consistent treatment of coherent and incoherent energy transfer dynamics using a variational master equation," *The Journal of Chemical Physics* **135**(11), 114501 (2011).
22. I. Kassal, J. Yuen-Zhou, and S. Rahimi-Keshari, "Does coherence enhance transport in photosynthesis?" *The Journal of Physical Chemistry Letters* **4**(3), 362–367 (2013).
23. I. Kassal and A. Aspuru-Guzik, "Environment-assisted quantum transport in ordered systems," *New J. Phys.* **14**(5), 053041 (2012).
24. M. Mohseni, A. Shabani, S. Lloyd, and H. Rabitz, "Energy-scales convergence for optimal and robust quantum transport in photosynthetic complexes," *The Journal of Chemical Physics* **140**(3), 035102 (2014).
25. P. Rebentrost, M. Mohseni, I. Kassal, S. Lloyd, and A. Aspuru-Guzik, "Environment-assisted quantum transport," *New J. Phys.* **11**(3), 033003 (2009).
26. A. Chin, J. Prior, R. Rosenbach, F. Caycedo-Soler, S. Huelga, and M. Plenio, "The role of non-equilibrium vibrational structures in electronic coherence and recoherence in pigment-protein complexes," *Nat. Phys.* **9**(2), 113–118 (2013).
27. R. Croce and H. Van Amerongen, "Natural strategies for photosynthetic light harvesting," *Nat. Chem. Biol.* **10**(7), 492–501 (2014).
28. H.-G. Duan, V. I. Prokhorenko, R. J. Cogdell, K. Ashraf, A. L. Stevens, M. Thorwart, and R. D. Miller, "Nature does not rely on long-lived electronic quantum coherence for photosynthetic energy transfer," *Proc. Natl. Acad. Sci.* **114**(32), 8493–8498 (2017).
29. D. M. Wilkins and N. S. Dattani, "Why quantum coherence is not important in the fenna–matthews–olsen complex," *Journal of Chemical Theory and Computation* **11**(7), 3411–3419 (2015).
30. S. D. Druger, S. Arnold, and L. M. Folan, "Theory of enhanced energy transfer between molecules embedded in spherical dielectric particles," *The Journal of Chemical Physics* **87**(5), 2649–2659 (1987).
31. T. Kobayashi, Q. Zheng, and T. Sekiguchi, "Resonant dipole-dipole interaction in a cavity," *Phys. Rev. A* **52**(4), 2835–2846 (1995).
32. M. Durach, A. Rusina, V. I. Klimov, and M. I. Stockman, "Nanoplasmonic renormalization and enhancement of Coulomb interactions," *New J. Phys.* **10**(10), 105011 (2008).
33. D. Martín-Cano, L. Martín-Moreno, F. J. García-Vidal, and E. Moreno, "Resonance energy transfer and superradiance mediated by plasmonic nanowaveguides," *Nano Lett.* **10**(8), 3129–3134 (2010).
34. V. N. Pustovit and T. V. Shahbazyan, "Resonance energy transfer near metal nanostructures mediated by surface plasmons," *Phys. Rev. B* **83**(8), 085427 (2011).
35. V. K. Komarala, A. L. Bradley, Y. P. Rakovich, S. J. Byrne, Y. K. Gun'ko, and A. L. Rogach, "Surface plasmon enhanced Förster resonance energy transfer between the CdTe quantum dots," *Appl. Phys. Lett.* **93**(12), 123102 (2008).
36. J. Zhang, Y. Fu, and J. R. Lakowicz, "Enhanced Förster resonance energy transfer (FRET) on a single metal particle," *The Journal of Physical Chemistry C* **111**(1), 50–56 (2007).
37. P. Andrew and W. L. Barnes, "Förster energy transfer in an optical microcavity," *Science* **290**(5492), 785–788 (2000).
38. C. Blum, N. Zijlstra, A. Lagendijk, M. Wubs, A. P. Mosk, V. Subramaniam, and W. L. Vos, "Nanophotonic Control of the Förster Resonance Energy Transfer Efficiency," *Phys. Rev. Lett.* **109**(20), 203601 (2012).
39. L. Zhao, T. Ming, L. Shao, H. Chen, and J. Wang, "Plasmon-Controlled Förster Resonance Energy Transfer," *The Journal of Physical Chemistry C* **116**(14), 8287–8296 (2012).
40. F. T. Rabouw, S. A. den Hartog, T. Senden, and A. Meijerink, "Photonic effects on the förster resonance energy transfer efficiency," *Nat. Commun.* **5**(1), 3610 (2014).
41. T. U. Tumkur, J. K. Kitur, C. E. Bonner, A. N. Poddubny, E. E. Narimanov, and M. A. Noginov, "Control of förster energy transfer in the vicinity of metallic surfaces and hyperbolic metamaterials," *Faraday Discuss.* **178**, 395–412 (2015).
42. D. L. Andrews and A. A. Demidov, *Resonance Energy Transfer* (Wiley, 1999).

43. H. T. Dung, L. Knöll, and D.-G. Welsch, "Intermolecular energy transfer in the presence of dispersing and absorbing media," *Phys. Rev. A* **65**(4), 043813 (2002).
44. H. T. Dung, L. Knöll, and D.-G. Welsch, "Resonant dipole-dipole interaction in the presence of dispersing and absorbing surroundings," *Phys. Rev. A* **66**(6), 063810 (2002).
45. A. Olaya-Castro, C. F. Lee, F. F. Olsen, and N. F. Johnson, "Efficiency of energy transfer in a light-harvesting system under quantum coherence," *Phys. Rev. B* **78**(8), 085115 (2008).
46. M. Mohseni, P. Rebentrost, S. Lloyd, and A. Aspuru-Guzik, "Environment-assisted quantum walks in photosynthetic energy transfer," *The Journal of Chemical Physics* **129**(17), 174106 (2008).
47. W. K. Wootters, "Entanglement of formation of an arbitrary state of two qubits," *Phys. Rev. Lett.* **80**(10), 2245–2248 (1998).
48. C. L. Cortes and Z. Jacob, "Super-coulombic atom–atom interactions in hyperbolic media," *Nat. Commun.* **8**(1), 14144 (2017).
49. A. Mahmoud, I. Liberal, and N. Engheta, "Dipole-dipole interactions mediated by epsilon-and-mu-near-zero waveguide supercoupling," *Opt. Mater. Express* **7**(2), 415–424 (2017).
50. S.-A. Biehs and G. Agarwal, "Qubit entanglement across ϵ -near-zero media," *Phys. Rev. A* **96**(2), 022308 (2017).
51. L.-P. Yang, H. X. Tang, and Z. Jacob, "Concept of quantum timing jitter and non-markovian limits in single-photon detection," *Phys. Rev. A* **97**(1), 013833 (2018).
52. S. Y. Buhmann and S. Scheel, "Macroscopic quantum electrodynamics and duality," *Phys. Rev. Lett.* **102**(14), 140404 (2009).